

# Light Tissue Interaction Study on Skin Tissue Using Monte Carlo Stimulation Method

<sup>1</sup>Jim Elliot Christopherjames, <sup>2</sup>Nithiyaa <sup>3</sup>Dharshini M, Srinithi G

Department of Biomedical Engineering,  
Saveetha Engineering College,  
Anna University, Chennai

## Abstract

The application of Monte Carlo simulation in the study of light-tissue interaction within skin tissue holds great significance in the realm of skin cancer research. This computational method offers a systematic approach to model the intricate interplay of light with various skin layers, enabling a profound understanding of photon behavior.

**Objective:** To analyze the impact of varying incident light parameters on the penetration depth and energy in skin tissue. To develop a robust Monte Carlo simulation model for accurately representing the propagation of skin tissue, accounting for scattering, absorption and reflection.

**Methods:** Monte Carlo stimulation stochastic random process in which light transport in tissues and their interactions can be studied effectively similar to other conventional applications

**Result :** The application of Monte Carlo simulation helped us to investigate light-tissue interaction within skin tissue has provided valuable insights into the complexities of skin cancer diagnostics and treatment. The knowledge derived from this research has the potential to revolutionize the field of skin cancer management, offering non-invasive diagnostic tools and precise therapeutic approaches.

**Conclusion:** Moving forward, the outcomes of this study are poised to make a substantial impact, paving the way for improved patient outcomes, early intervention, and enhanced quality of life for individuals affected by skin cancer. Through meticulous modeling of photon behavior, we have advanced our understanding of how light can be harnessed for early detection and targeted therapies.

**Keywords:** Monte Carlo, phantom, optical properties of light, skin tissue

## 1. Introduction

Skin cancer is a pressing worldwide health concern, with its gradually increasing incidence over the years. Understanding the interaction between light and skin tissue is of paramount importance in the context of both diagnosis and treatment of skin cancer. This intricate relationship can be effectively explored through the application of the Monte Carlo simulation method, a powerful computational technique.

Various forms of skin cancer are manifested, each with its distinctive characteristics and behaviours. The three main types—basal cell carcinoma (BCC), squamous cell carcinoma (SCC), and melanoma—paint a diverse mosaic of malignancies, ranging

from slow-growing, localized lesions to aggressive, metastatic tumors.

BCC, often considered the most common type, is typically manifested as a flesh-coloured or pearly bump, often mistaken for a benign growth. While it tends to grow slowly and rarely undergoes metastasis, the need for early detection and intervention is underscored by its prevalence. SCC, on the other hand, emanates from the squamous cells in the skin's upper layers. Manifesting as red, scaly patches or open sores, SCC exhibits a higher propensity for metastasis compared to BCC, necessitating vigilant monitoring and treatment.

Melanoma, the most notorious member of the skin cancer trio, arises from the pigment-producing melanocytes. Characterized by its potential for

rapid spread, melanoma demands immediate attention due to its heightened metastatic risk. Early detection becomes a lifeline in the face of melanoma's aggressive nature.

The use of random sampling and probability is involved in modelling complex systems. In our case, it is employed to simulate how light, in various forms, interacts with the layers of human skin. This simulation allows us to comprehend the dynamic behaviour of photons within the skin tissue, providing insights into the scattering, absorption, and reflection of light. Monte Carlo simulation meticulously calculates each photon's journey through the skin tissue.

The goal of this research is to delve deeply into the underlying physics of light-tissue interaction, aiming to enhance our understanding of skin cancer diagnostics and therapy.

Light, a vital element in our daily lives, can also be harnessed for the betterment of healthcare. In skin cancer diagnosis, optical techniques, such as spectroscopy and imaging, have gained prominence. Valuable information about the tissue's health is provided by these techniques, relying on the interaction of light with skin tissue.

## **2. Materials and Methods**

### **A. Monte Carlo Simulation**

Monte Carlo simulation (MCS) is a stochastic random process in which light transport in tissues and their interactions can be studied effectively similar to other conventional applications [18]–[20]. The neutral light photons enter the tissue surface perpendicularly so that maximum energy can be utilized. The light photons used in this study are 1 million photons in number and the beam shape is infinitely narrow. There exhibits a random movement and interaction of light photons [21]–[24]. The optical parameters of interest include absorption coefficient  $\mu_a$  ( $\text{cm}^{-1}$ ), scattering coefficient  $\mu_s$

( $\text{cm}^{-1}$ ), refractive index ( $n$ ), and anisotropy factor ( $g$ ). The light photon enters the tissue medium with an initial weight of 1 and it undergoes multiple interactions inside the medium and emerges either at the top ( $x$ -direction) surface or the bottom ( $z$ -direction) surface or the photons are lost due to multiple interactions hence absorbed respectively. The simulation technique has been efficiently

applied using the C++ programming language. The flowchart of the MCS can be found elsewhere [14]. A storage 2D grid element is created so that all the detected photons are stored. Initial photon step size is set and it is incident on the tissue surface for interaction. The variable step size of the light photon was estimated using a generated random variable. As the photon interacts with tissue compositional elements, the path length was found, and thereafter it was moved. For all the subsequent movements, the detector positions were checked for the presence of detected photons. If the photons were detected, a counter was set to increment the photon received by the corresponding detector. If the photons were internally reflected, then the photon location was updated and the simulation process was continued. There is a reduction in the photon weight proportionally at each step, due to absorption and scattering by the tissue. The amount of weight lost  $Q$ , in absorption was given by  $\delta Q = W$  where  $W$  represents the total weight of the photon. The photon weight and direction after scattering were updated. The new position of the photon ( $x'$ ,  $y'$ ,  $z'$ ) from the previous position ( $x$ ,  $y$ ,  $z$ ) was indicated. If the photon weight falls below a minimum threshold ( $= 0.001$ ), it is subjected to roulette conditions for elimination. If the condition is satisfied, an updated step is set and the process starts from the beginning. The photon is terminated and the detector recognizes the number of photons and the position of exit. The entire process is repeated for several number of light photons. The unique advantage of Monte Carlo simulation is its ability to model a wide spectrum of scenarios, mirroring the diverse ways light is employed in medical applications. By carefully crafting the simulation parameters, we can investigate the impact of different wavelengths, incident angles, and skin types on the outcome. It's akin to a director experimenting with lighting, camera angles, and actors to achieve the perfect shot. Moreover, the accuracy and versatility of Monte Carlo simulations enable researchers to explore the effects of varying skin conditions, including melanoma, squamous cell carcinoma, and basal cell carcinoma. Just as a director works with different actors to portray various characters, this simulation can adapt to the characteristics of different skin types, offering a

comprehensive view of how light interacts with each. The knowledge gained from this research is invaluable for skin cancer diagnosis and treatment. For diagnosis, it helps in developing non-invasive, optical diagnostic tools that can differentiate between healthy and cancerous tissue. Just as a director crafts a compelling narrative, understanding light-tissue interaction can lead to a powerful story of early detection and improved patient outcomes.

### B. Optical hand held Scanner

The handheld numerical optical scanner is made up of two probes: the Dual Side Detector (DSD) probe and the Single Source Detector (SSD) probe. Comprised of a single **source** emitting light through the numerical phantom, and 21 detectors arranged to collect light from the incident surface; the DSD probe is illustrated schematically in Fig. 1a, with red representing the source and green representing the detectors. While having a total of 21 detectors including 10 on each side as well as one at the source, all of which are spaced uniformly at an inter-detector distance of 1 mm centre-to-centre. For example, the photon collection radius for each detector was set at 0.5 mm.

Fig. 1b shows an SSD probe with one source followed by more than one detector. The first detector is separated from the source by a centre-to-centre distance of 2 mm while subsequent detectors are separated by 1 mm from each other. In this study, several Source-Detector (SD) separations consisting of 2,3,4,5,6,7,8 and 9 mm were used. The radius of both the source and detector is set at 0.5mm in this case.

256x256 pixels; 16-bit; 128K

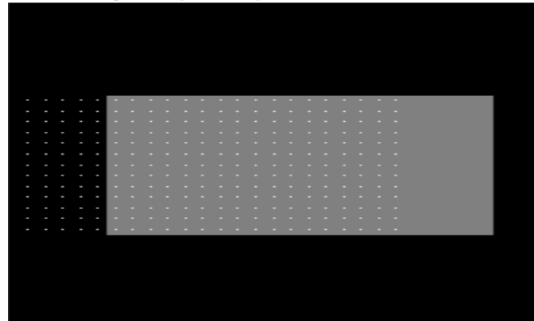


Fig 1a : Optical handheld scanner

### C. Numerical phantoms

Numerical phantoms resembling biological human skin tissues were generated in this study. The

simulation code exhibits versatility in constructing numerical phantoms of variable dimensions, incorporating inclusions of diverse shapes and sizes across multiple layers. These phantoms were formulated based on their respective optical properties. Table 1 provides details on the optical properties of normal (non-cancerous) adipose, epidermis, and dermis, as well as abnormal (cancerous) tissues. The numerical phantoms created were single, double, and multi-layered, with and without embedded inclusions of abnormal tissues.

The aforesaid phantoms in the three categories were created to conduct experiments using SSD and DSD probes. Phantoms without inclusions are referred to as normal, whereas those with inclusions are referred to as abnormal.

Table 1: Optical Properties

Sl. No	Tissues	Wave length, $\lambda$ (nm)	Optical properties			
			$\mu_a$	$\mu_s$	G	n
1.	Epidermis	700	1.06	54.66	0.8	1.3
2.	Dermis	700	0.52	53.62	0.71	1.3
3.	Sub dermis	700	0.09	0.01	0.69	1.3
4.	adipose	700	1.11	0.01	0.66	1.4
5.	Blood	700	0.75	80	0.98	1.3
6.	Melanoma	700	6.55	19.1	0.9	1.4

### D. Data acquisition

Experimentally, we obtained data using Dual Side Detector (DSD) and Single Source Detector (SSD) probes to acquire measurements from both normal and abnormal number phantoms. The Monte Carlo simulation consisted of 1 million photons of light falling on the source position with detectors capturing backscattered photons along the x-direction in the DSD probe on both sides of the source. The collected photons were recorded at corresponding positions on a  $256 \times 256 \times 256$  grid that represented the physical dimensions of the phantom being used in this case ( $30 \times 30 \times 30$  mm). To put it simply, while scanning along specified detector grids, the probe quantified how many detected photons occurred simultaneously.

The SSD probe was moving linearly over coordinates  $(-x,0,0)$  to  $(x,0,0)$  at 1mm interval. At each step of scan, one million incident photons were present at source's position and its back scattered ones was detected by all detectors simultaneously. Backscattered photons from single tissue normal phantoms consisting of ductal carcinoma, fibrocystic and glandular tissues were collected using the DSD probe at 800 nm. Data were then obtained from the first set of phantoms as shown in Fig. 3a and b by using the DSD probe with sources operating at 600 and 800 nm. The SSD probe for its part captured backscattered photons from the same phantoms having spherical and disc shaped inclusions with a source operating at 800 nm. Using both DSD and SSD probes, data was additionally obtained from a double-layer phantom containing a spherical-shaped ductal carcinoma inclusion at a depth of 8 mm. Also, using the SSD probe backscattered photons were recorded from a multi-layer phantom with a disc-shaped ductal carcinoma inclusion at a depth of 5.75 mm. Each Source-Detector (SD) configuration's data files were stored separately from those obtained by the SSD probe. During all these experiments five iterations have been carried out and each time separate files for backscattered photons collected were created.

#### **E. Data processing**

The collected backscattered photons by both DSD and SSD probes underwent an averaging process across different iterations to mitigate noise. Data from normal phantoms across three categories were classified as background data, while those from abnormal phantoms were categorized as foreground data. Subsequently, background data were subtracted from foreground data after averaging. The resultant data were normalized by the total photon count, yielding the percentage of normalized backscattered intensity (NBI %), as described by Srinivasan et al. (2004). To further refine the dataset, a Gaussian filter with a window size of  $22 \times 22$  was applied for smoothing. This standardized procedure was consistently applied across all measurements. Finally, the processed data from all measurements were represented graphically as signals.

### **3. Results and Discussions**

Optical sources like lasers and LEDs find extensive utility in medical fields for both diagnostic and therapeutic purposes. Particularly in near-infrared applications, these sources can penetrate deep into tissues, offering valuable insights into underlying layers through backscattering and light energy transmission. The effectiveness of this penetration is contingent upon the optical characteristics of the tissues, with light absorption decreasing as wavelength increases. This study demonstrated that light photons at 600 nm were unable to penetrate beyond superficial layers, primarily due to absorption and scattering within the tissue, leading to a diminished number of received photons.

Monte Carlo simulation serves as a suitable model for the random path of light photons through tissues. In this study, two probes were simulated to emit and receive light photons from numerical phantoms of human breast tissue, based on their optical properties. Despite receiving minimal signals, these probes successfully identified the presence and location of a 2 mm melanoma amidst surrounding subcutaneous tissue, as inferred from the intensity of the received signals ( $|PI|$ ). However, the Full Width at Half Maximum (FWHM) derived from the signals did not correspond to the size of the melanoma, likely due to dominant scattering within the medium and the melanoma's location. With increasing melanoma size, FWHM increased proportionately with its depth.

While the FWHM did not directly correlate with melanoma size, the  $|PI|$  indirectly indicated size differences, with larger sizes exhibiting higher amplitude compared to smaller ones at the same depth. Despite the low signal amplitudes attributed to distance, the simulated probes could detect thin layers of embedded malignant tissues of various sizes, showcasing their potential for early malignancy detection. Furthermore, the study suggested that these probes could detect embedded tissues within multilayer tissue structures, indicating their potential for superficial malignancy detection in human skin tissue and potential utilization in large-scale screening programs.

Total of 3,00,000 photons were generated in both background and foreground respectively. They were further averaged and blended to obtain the final

image which was further enhanced using gaussian filter.

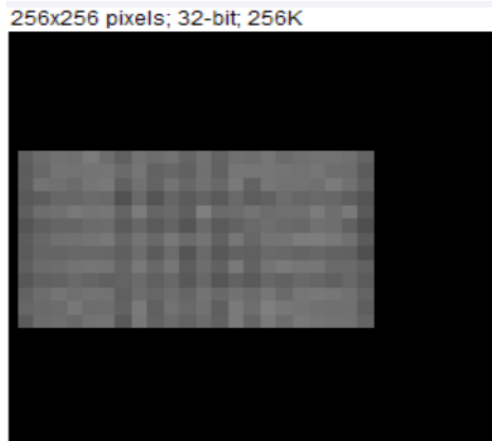


Fig 1b: Background phantoms.

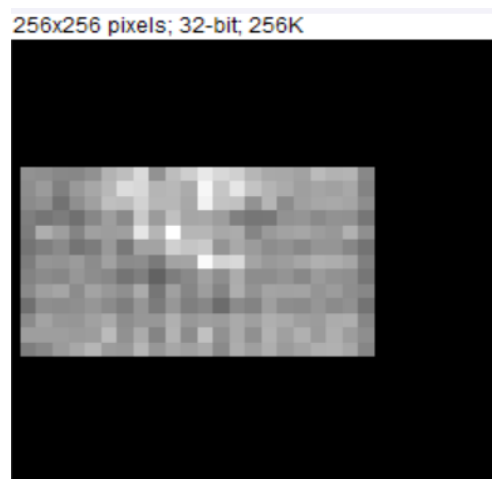


Fig 1c: Foreground Phantoms.



Fig 1d: Blended image of FG and BG.

Observing the results obtained from backscattering, it is evident that the simulated probe could be used to detect and diagnose the presence of melanoma

even at a depth of 2 mm. The photons with the wavelength of 800 nm could penetrate deeper and the embedded tissues were seen from the obtained signals. The results obtained show that a similar handheld optical imager for human tissue imaging could be successfully developed to detect malignancy in the human skin tissue.

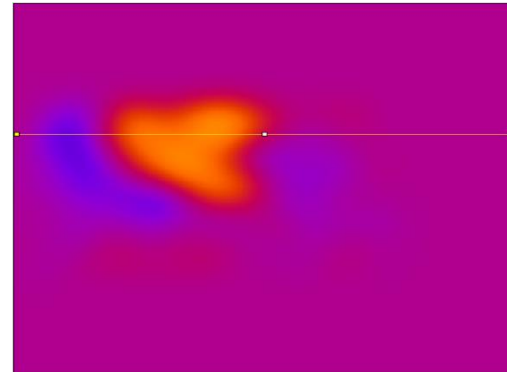


Fig 1e: Presence of melanoma in the probe view

The Monte Carlo simulation method has proven to be an effective tool for modelling the random path of light photons through skin tissue. By simulating the interaction of light with skin tissue, we can better understand the underlying mechanisms and optimize the design of optical probes and devices for various medical applications. Expected raw phantoms are 12.5 and generated phantoms are 9.37. The error or difference in phantoms is estimated up to 33.40%.

#### 4. Conclusion

In conclusion, the application of Monte Carlo simulation to investigate light-tissue interaction within skin tissue has provided valuable insights into the complexities of skin cancer diagnostics and treatment. Through meticulous modelling of photon behaviour, we have advanced our understanding of how light can be harnessed for early detection and targeted therapies. The knowledge derived from this research has the potential to revolutionize the field of skin cancer management, offering non-invasive diagnostic tools and precise therapeutic approaches. As we move forward, the outcomes of this study are poised to make a substantial impact, paving the way for improved patient outcomes, early intervention, and enhanced quality of life for individuals affected by skin cancer.

## References

- [1] Sathya, T. Deepan, C. Jim Elliot, and J. B. Jeeva, "Development and phantom study on near-infrared diffuse optical tomographic imager," in *Materials Today: Proceedings*, vol. 15. Elsevier Ltd, Jan 2019, pp. 309–315.
- [2] S. L. Jacques, "Optical properties of biological tissues: A review," p. R37, Jun 2013. [Online]. Available: <https://iopscience.iop.org/article/10.1088/0031-9155/58/11/R37>  
<https://iopscience.iop.org/article/10.1088/0031-9155/58/11/R37/meta>
- [3] Y. Hasegawa, Y. Yamada, M. Tamura, and Y. Nomura, "Monte Carlo simulation of light transmission through living tissues," *Applied Optics*, vol. 30, no. 31, p. 4515, Nov 1991. [Online]. Available: <https://www.osapublishing.org/viewmedia.cfm?uri=ao-30-31-4515&seq=0&html=true>  
<https://www.osapublishing.org/abstract.cfm?uri=ao-30-31-4515>
- [4] J. B. Jeeva and M. Singh, "Reconstruction of optical scanned images of inhomogeneities in biological tissues by Monte Carlo simulation," *Computers in Biology and Medicine*, vol. 60, pp. 92–99, May 2015.
- [5] Optical parameters of embedded abnormalities in tissues as determined by Monte Carlo simulation," *Electromagnetic Biology and Medicine*, vol. 31, no. 3, pp. 204–212, Sep 2012. [Online]. Available: <https://www.tandfonline.com/doi/abs/10.3109/15368378.2012.700296>
- [6] P. S. Pandian, M. Kumaravel, and M. Singh, "Multilayer imaging and compositional analysis of human male breast by laser reflectometry and Monte Carlo simulation," *Medical and Biological Engineering*
- [7] T. Kono, J. Yamada In vivo measurement of optical properties of human skin for 450–800 nm and 950–1600 nm wavelengths *Int. J. Thermophys.*, 40 (2019), pp. 1–14, 10.1007/s10765-019-2515-3
- [8] Krasnikov et al., 2019 I. Krasnikov, A. Seteikin, B. Roth, *Advances in the simulation of light–tissue interactions in biomedical engineering*, *Biomed. Eng. Lett.* 2019 93. 9 (2019) 327–337.
- [9] S. Kumari, A.K. Nirala Study of light propagation in human, rabbit and rat liver tissue by Monte Carlo simulation
- [10] S. Kumari, A.K. Nirala Study of light propagation in human and animal tissues by Monte Carlo simulation
- [11] Karimkhani C, Boyers LN, Dellavalle RP, Weinstock MA. It's time for "keratinocyte carcinoma" to replace the term "nonmelanoma skin cancer". *J Am Acad Dermatol.* 2015;72(1):186–7.
- [12] Rogers HW, Weinstock MA, Harris AR, Hinckley MR, Feldman SR, Fleischer AB, et al. Incidence estimate of nonmelanoma skin cancer in the United States, 2006. *Arch Dermatol.* 2010;146(3):283–7.
- [13] Asgari MM, Moffet HH, Ray GT, Quesenberry CP. Trends in basal cell carcinoma incidence and identification of high-risk subgroups, 1998–2012. *JAMA Dermatol.* 2015;151(9):976–81.
- [14] Miller DL, Weinstock MA. Nonmelanoma skin cancer in the United States: incidence. *J Am Acad Dermatol.* 1994;30(5 Pt 1):774–8.
- [15] Jambusaria-Pahlajani A, Kanetsky PA, Karia PS, Hwang W-T, Gelfand JM, Whalen FM, et al. Evaluation of AJCC tumor staging for cutaneous squamous cell carcinoma and a proposed alternative tumor staging system. *JAMA Dermatol.* 2013;149(4):402–10.
- [16] Stevenson ML, Kim R, Meehan SA, Pavlick AC, Carucci JA. Metastatic cutaneous squamous cell carcinoma: the importance of T2 stratification and hematologic malignancy in prognostication. *Dermatol Surg.* 2016;42(8):932–5.
- [17] Bologna JL, Jorizzo JL, Schaffer JV. *Dermatology*. 3rd ed. Philadelphia: Elsevier Saunders; 2012.
- [18] Alguire PC, Mathes BM. Skin biopsy techniques for the internist. *J Gen Intern Med.* 1998;13(1):46–54. 12 Procedures in the Diagnosis and Treatment of Skin Cancer 264.
- [19] Miedema J, Zedek DC, Rayala BZ, Bain EE. 9 tips to help prevent derm biopsy mistakes. *J Fam Pract.* 2014;63(10):559–64.

- [20] Stratman EJ, Elston DM, Miller SJ. Skin biopsy: identifying and overcoming errors in the skin biopsy pathway. *J Am Acad Dermatol.* 2016;74(1):19–25. quiz 25.
- [21] Steinsapir KD, Woodward JA. Chlorhexidine keratitis: safety of chlorhexidine as a facial antiseptic. *Dermatol Surg.* 2017;43(1):1–6.
- [22] Rowe DE, Carroll RJ, Day CL. Long-term recurrence rates in previously untreated (primary) basal cell carcinoma: implications for patient follow-up. *J Dermatol Surg Oncol.* 1989;15(3):315–28.
- [23] Barlow JO, Zalla MJ, Kyle A, DiCaudo DJ, Lim KK, Yiannias JA. Treatment of basal cell carcinoma with curettage alone. *J Am Acad Dermatol.* 2006;54(6):1039–45.
- [24] Goldman G. The current status of curettage and electrodesiccation. *Dermatol Clin.* 2002;20(3):569–78. ix
- [25] Kauvar ANB, Arpey CJ, Hruza G, Olbricht SM, Bennett R, Mahmoud BH. Consensus for nonmelanoma skin cancer treatment, part II: squamous cell carcinoma, including a cost analysis of treatment methods. *Dermatol Surg.* 2015;41(11):1214–40.
- [26] Zitelli JA. TIPS for a better ellipse. *J Am Acad Dermatol.* 1990;22(1):101–3.
- [27] Thissen MR, Neumann MH, Schouten LJ. A systematic review of treatment modalities for primary basal cell carcinomas. *Arch Dermatol.* 1999;135(10):1177–83.
- [28] Bichakjian CK, Olencki T, Aasi SZ, Alam M, Andersen JS, Berg D, et al. Basal cell skin cancer, version 1.2016, NCCN clinical practice guidelines in oncology. *J Natl Compr Canc Netw.* 2016;14(5):574–97.
- [29] Wolf DJ, Zitelli JA. Surgical margins for basal cell carcinoma. *Arch Dermatol.* 1987;123(3):340–4.
- [30] Brodland DG, Zitelli JA. Surgical margins for excision of primary cutaneous squamous cell carcinoma. *J Am Acad Dermatol.* 1992;27(2 Pt 1):241–8.